ELSEVIER

Ceramics International 29 (2003) 455–462

CERAMICS
INTERNATIONAL

www.elsevier.com/locate/ceramint

The effect of SiO_2 and Cr_2O_3 additions on the crystallisation behaviour and magnetic properties of a B_2O_3–BaO–Fe_2O_3 glass

V.K. Marghussian*, A. Beitollahi, M. Haghi

Ceramics Division, Department of Materials, Iran University of Science and Technology, Narmak, Tehran 16844, Iran

Received 30 May 2002; received in revised form 25 June 2002; accepted 2 September 2002

Abstract

Differential thermal analysis, X-ray diffractometry and scanning electron microscopy with energy dispersive spectroscopy were used to study the crystallisation of a glass with a composition of 45% BaO, 30% B_2O_3 and 25% Fe_2O_3 (mol%), to which 10–30% SiO_2 was added replacing B_2O_3. The effect of 1 mol% Cr_2O_3 as a nucleation agent also was studied. The magnetic properties of some specimens also were measured with a vibrating sample magnometer. It was found that while the addition of >10 mol% SiO_2 prevented formation of barium hexaferrite, the main magnetic phase, Cr_2O_3, greatly enhanced surface crystallisation. All specimens revealed glass in-glass phase separation, which in the presence of Cr_2O_3 was more extensive and on a much finer scale. The latter specimens, in the form of pressed glass frits heat treated 1 h at 723 °C, showed a coercive force of $H_c=4150$ Oe and saturation magnetisation of $M_s=9.92$ emu/g.

Keywords: C. Magnetic properties; D. Glass ceramics; D. Ferrites; E. Hard magnets

1. Introduction

Barium hexaferrite($BaFe_{12}O_{19}$) has been widely used in permanent magnets, both in sintered and plastic forms. Furthermore barium ferrite particulate media have been utilised as promising high-density recording media in fields ranging from audio and video records to flexibe disk memories. The glass-crystallisation method has also attracted considerable attention as a suitable means to prepare hexafrrite magnetic materials [1–13]. From the point of view of controlling the microstructure, the glass-ceramic method in general is superior to usual ceramic fabrication process by solid-state reaction. In the glass-ceramic method very small and strainfree crystals having the desired size and shape can be obtained by the controlled crystallisation. The glass-ceramic route can be used to prepare both bulk magnetic materials and particulate media. In the latter case, the amorphous phase is usually leached out of the glass-ceramic specimens. Many aspects of the glass-ceramic process, including the effect of composition, nucleating agents and heat treatment schedule upon magnetic properties have been investigated [1–13].

In this study the effect of Cr_2O_3 and SiO_2 additions on the crystallisation behaviour and magnetic properties of bulk glass-ceramics in the B_2O_3–BaO–Fe_2O_3 system was investigated. To the authors knowledge no reports concerning the effect of Cr_2O_3 as a nucleant in the glasses of this system appear in the literature.

2. Experimental procedure

The glass compositions were prepared by melting the required amounts of reagent grade chemicals ($BaCO_3$, H_3BO_3, Fe_2O_3, Cr_2O_3 and pure quartz sand) in alumina or zircon crucibles at 1250–1300 °C for 1–2 h in an electrically heated furnace. The glass melts were either cast into preheated steel moulds or quenched into distilled water. Dilatometric softening points (T_d) and crystallisation temperatures (T_c) were estimated from differential thermal analysis (DTA) plots obtained on a Cambridge STA (model 1640) Instrument. The heating rate was 20 °C min^{-1} and alumina was used as an inert reference material.The shifts of crystallisation (exothermic) peaks (ΔT),

---

* Corresponding author. Fax: +98-21-7454057.
E-mail address: v_k_marghus@yahoo.com (V.K. Marghussian).

0272-8842/03/$30.00 © 2003 Elsevier Science Ltd and Techna S.r.l. All rights reserved.
PII: S0272-8842(02)00187-6

upon changing the DTA sample particle sizes in the <53 μm to the 0.5–0.6 mm range also were measured. The samples were then heat treated at their corresponding crystallisation temperatures for different time periods and the crystalline phases developed after heat treatment were identified by X-ray powder diffraction (XRD) method utilizing a Jeol (JDX-8030) diffractometer.The microstructures were observed with a scanning electron microscope (Cambridge SEM model 360), using polished sections. The specimens were etched in a solution of 0.1 M HF and 0.05 M HCl for 30 s before coating with a thin film of gold. The saturation magnetisation (M_s) and coercivity (H_c) were determined with a vibrating sample magnetometer.

3. Results and discussion

3.1. Differential thermal analysis and X-ray diffraction

Table 1 shows the glass compositions investigated in this work. As the DTA results shown in Table 2 indicate, the base glass composition (BC) was not suitable for bulk crystallisation because of its weak exothermic effect. Therefore it was decided to add 1 mol% Cr_2O_3 as a nucleant to the glass composition (sample BC1). It can be seen that this specimen exhibited relatively small ΔT values indicating a marked bulk crystallisation ability (Table 2). The melts of composition BC1, owing to their strong crystallisation tendency, showed some signs of crystallisation even during the casting operation. To prevent this it was decided to add 10–30 mol% SiO_2 at the expense of B_2O_3 to the base composition. (Table 1 specimens BS-10 to BS-30).

DTA traces of the earlier mentioned samples showed the appearance of multiple exo-peaks and considerable ΔT (peak shift) values (Table 2). The DTA peak shifts of fine particle size specimens towards lower temperatuers (relative to the coarse particle size specimens), is an indication of the prevalence of surface crystallisation over bulk crystallisation. XRD results summarised in Table 3 show the crystallisation products after heat treating the specimens at their respective DTA exo-peaks for the indicated time periods. It can be seen that in specimens BS20 and BS30 there is no sign of $BaFe_{12}O_{19}$ after crystallisation and in specimen BS10 a silicate phase ($Ba_2FeSi_2O_7$) appeared together with the barium hexaferrite phase. It is interesting to note that the addition of 1 mol% Cr_2O_3 to BS10 resulted in disappearance of the exothermic effect from the DTA trace of coarse grain glass samples but the appearance of a relatively sharp peak in the trace of glass samples having a fine particle size. Fig. 1 shows some typical DTA traces. The Cr_2O_3 containing samples developed BaB_2O_4 and $BaFe_{12}O_{19}$ phases after crystallisation (Table 3). The peak heights of hexaferrite phase being the highest among the glass samples investigated in this work. Therefore it can be concluded that the addition of Cr_2O_3 either prevented the crystallisation of silicate phases or greatly assisted the surface crystallisation of

Table 1
Chemical compositions of glass samples

Sample	Chemical composition (mol%)				
	BaO	Ba_2O_3	Fe_2O_3	SiO_2	Cr_2O_3
BC	45	30	25	–	–
BC1	45	30	25	–	1
BS10	45	20	25	10	–
BS20	45	10	25	20	–
BS30	45	–	25	30	–
BSC1	45	20	25	10	1

Table 2
Dilatometric softening points, crystallisation temperatures and DTA peak shifts (ΔT) for various glass specimens

Specimen	Dilatometric softening point T_d (°C)	Crystallisation (exo) peak temp.(°C) for coarse (0.5–0.6 mm) samples	DTA peak shift values[a] (ΔT) °C
BC	548	No peak was detected for coarse grain sizes but weak effects were detected at 636 and 715 °C for fine grain samples.	–
BC1	514	679°, 809°	14.1, 17.6
BS10	581.6	665.2, 797.2, 871.3°	25.6, 92.3, 50.3
BS20	628.0	910.3°	74.6
BS30	656.5	850, 898, 950.7°	50 (for second peak)
BSC1	542	No peak was detected for coarse grain sizes but a sharp peak was detected for fine grain size samples at 723.4 °C	–

[a] for first, second & third peaks respectively

Table 3
Heat treatment conditions and XRD results for various specimens

Sample	Heat treatment temp (°C)	Heat treatment time (h)	Crystallisation products
BC1	679	3	Fe_2O_3,BaB_2O_4,$BaFe_{12}O_{19}$
BC1	809	3	BaB_2O_4,$BaFe_{12}O_{19}$
BS10	665	1	No crystalline phase detected.
BS10	797	1	$Ba_2FeSi_2O_7$,$BaFe_{12}O_{19}$
BS10	797	3	$Ba_2FeSi_2O_7$,$BaFe_{12}O_{19}$
BS10	797	5	$Ba_2FeSi_2O_7$,$BaFe_{12}O_{19}$
BS10	871	1	$Ba_2FeSi_2O_7$,$BaFe_{12}O_{19}$
BS10	871	3	$Ba_2FeSi_2O_7$,$BaFe_{12}O_{19}$
BS10	871	5	$Ba_2FeSi_2O_7$,$BaFe_{12}O_{19}$
BS20	910	1	$Ba_2FeSi_2O_7$,$BaSi_2O_5$
BS30	850	1	$Ba_2FeSi_2O_7$,$Ba_4B_2O_7$
BS30	898	1	$Ba_2FeSi_2O_7$,$Ba_4B_2O_7$
BS30	950	1	$Ba_2FeSi_2O_7$,$Ba_4B_2O_7$
BSC1	723	1	BaB_2O_4,$BaFe_{12}O_{19}$

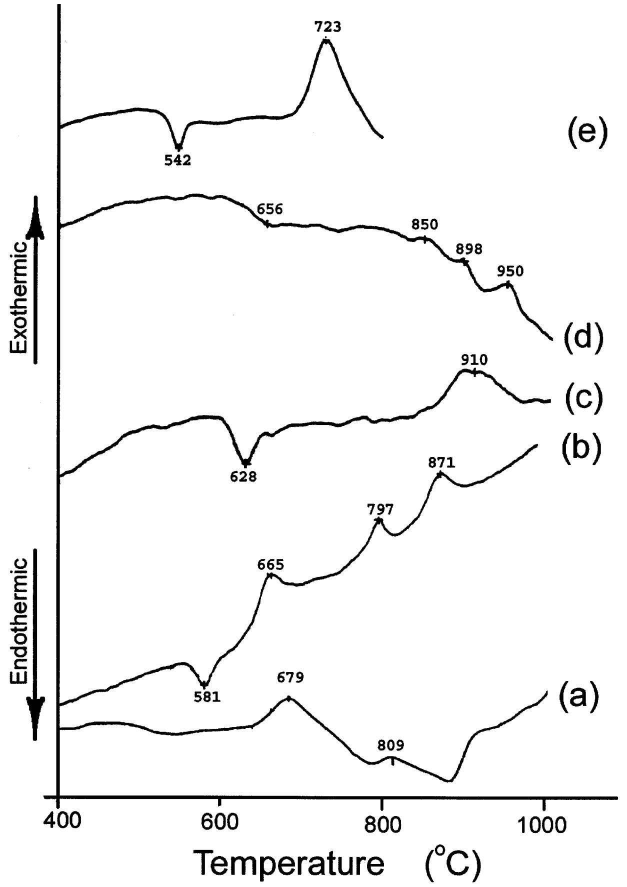

Fig. 1. DTA traces for (a) specimen BC1, (b) specimen BS10, (c) specimen BS20, (d) specimen BS30, (e) specimen BSC1.

barium hexaferrite phase or both. It can also be seen that Cr_2O_3 has reduced the viscosity of glass specimens containing 10% SiO_2 (compare the dilatometric softening points of specimens BS10 and BSC1, Table 2). This can also lead to faster crystallisation rates in Cr_2O_3 containing specimens.

3.2. Microstructural investigations

Figs. 2–4 show SEM micrographs of BS, BS10 and BSC1 glass samples respectively. It can be seen that while all specimens show extensive phase separation, the Cr_2O_3-containing specimens (BSC1) exhibit the finest microstructures, comprising a fine Fe_2O_3 rich phase (bright regions) dispersed in a continuous B_2O_3 and BaO rich phase (dark regions). The chemical make up of the phases, as characterized by energy dispersive spectroscopy (EDS) is shown in Fig. 5 (a & b). Therefore it can be concluded that Cr_2O_3 has enhanced the phase separation tendency of the B_2O_3–SiO_2–BaO–Fe_2O_3 glass samples probably by increasing the width of immiscibility region causing more distinct composional differences and a less durable borate rich phase. This may result in overall viscosity reduction, if the lower viscosity phase is the continuous phase [14]. (see Fig. 4 and compare dilatometric softening points of specimens BS10 and BSC1 in Table 2).

Fig. 6 shows a SEM image of specimen BSC1 after crystallisation at 723 °C for 1 h. Two apparently different morphological features can be seen, namely large

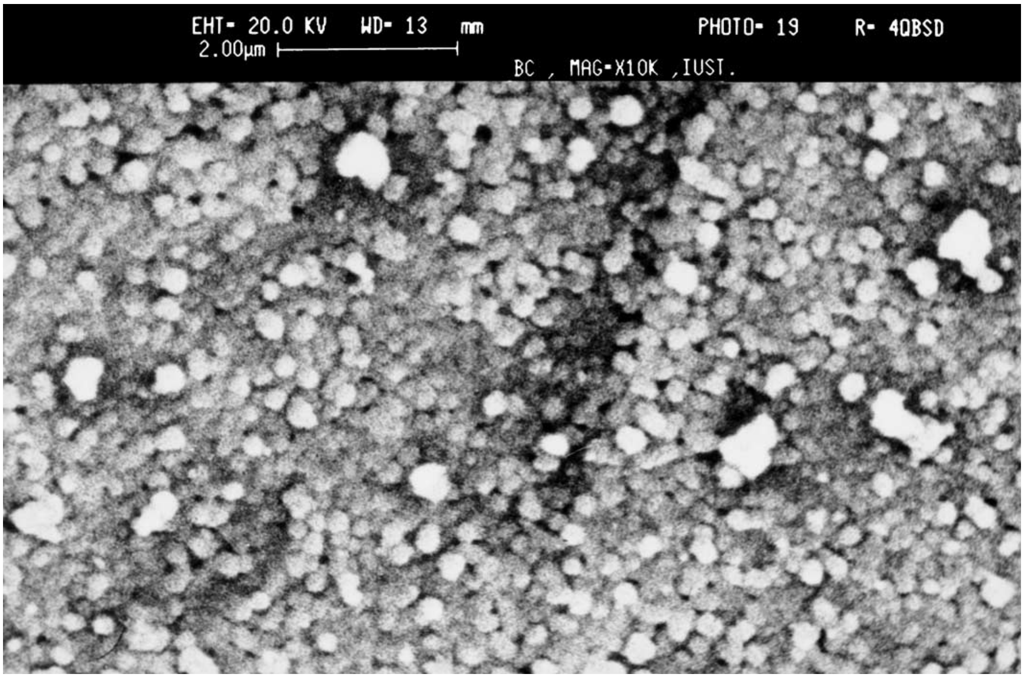

Fig. 2. SEM micrograph of glass sample BS showing phase separation (back scattered electron image).

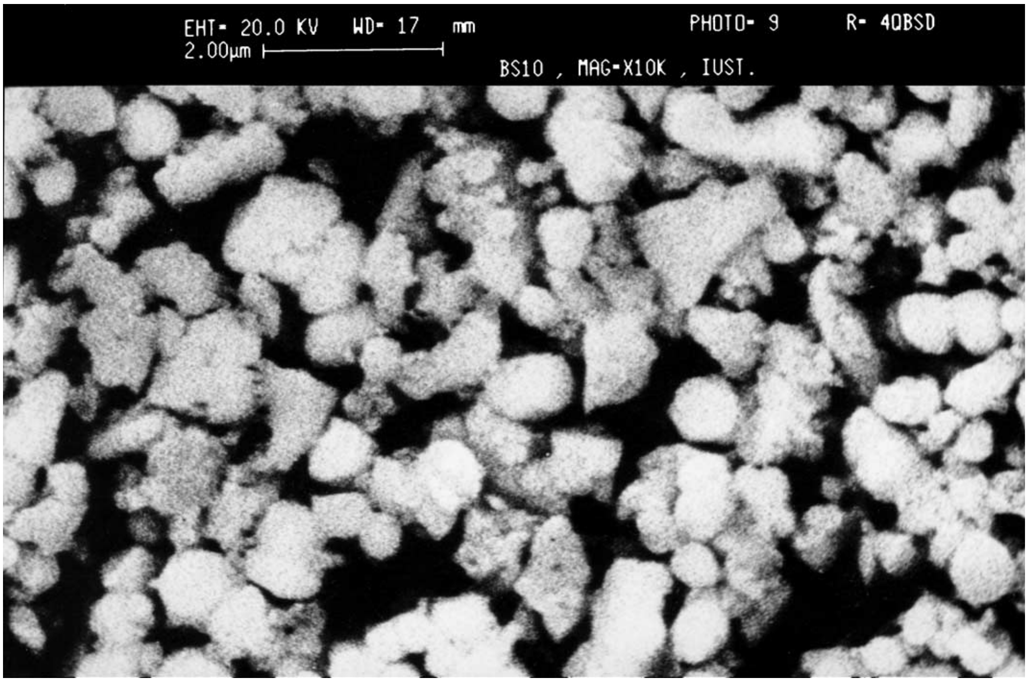

Fig. 3. SEM micrograph of glass sample BS10 (back scattered electron image).

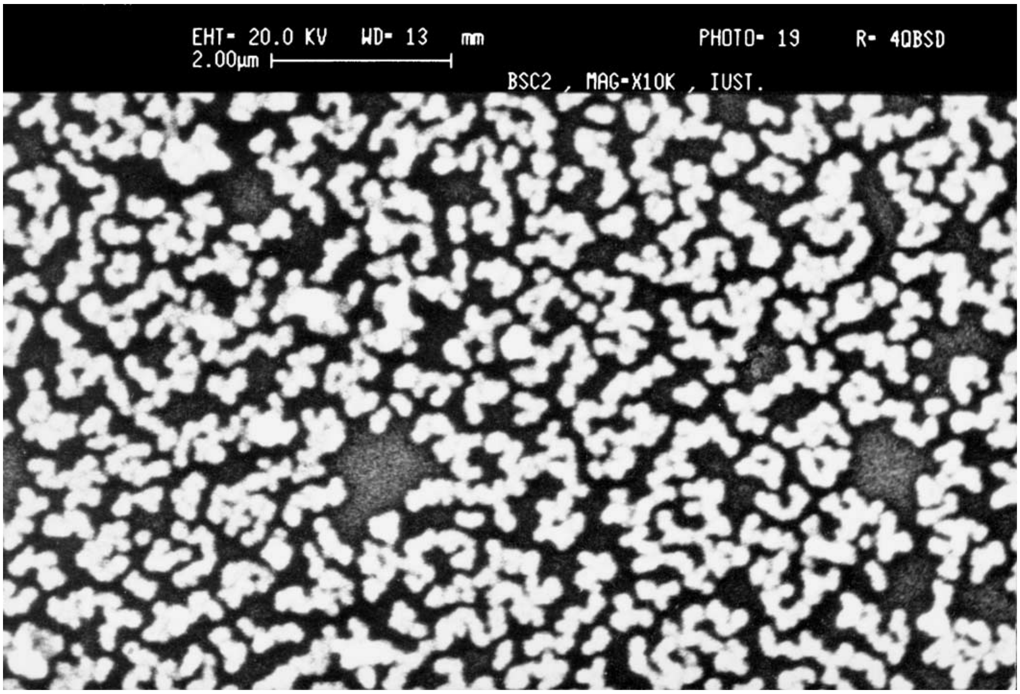

Fig. 4. SEM micrograph of glass sample BSC1 (back scattered electron image).

ellipsoidal particles and fine platelets. As the results of EDS shown in Fig. 7 revealed, the ellipsoidal particles are BaB_2O_4 and the fine platelets are $BaFe_{12}O_{19}$. (The only two phases present in BSC1 specimens after crystallisation, according to XRD results.) The presence of ellipsoidal particles probably indicate a spherulitic growth morphology for BaB_2O_4. Spherulites which commenly occur in organic polymers, some silicate minerals and glasses [15–17] are generally composed of radially oriented fibres. There are different types of spherulites, some of which appear as spheres and ellipsoids [15]. Fig. 8 shows an enlarged micrograph of the latter particles. It can be seen that some $BaFe_{12}O_{19}$ platelets are growing at the surface of ellipsoids. Fig. 6 also exhibits the presence of some platelets at the surface or adjacent to ellipsoidal particles. It seems that $BaFe_{12}O_{19}$

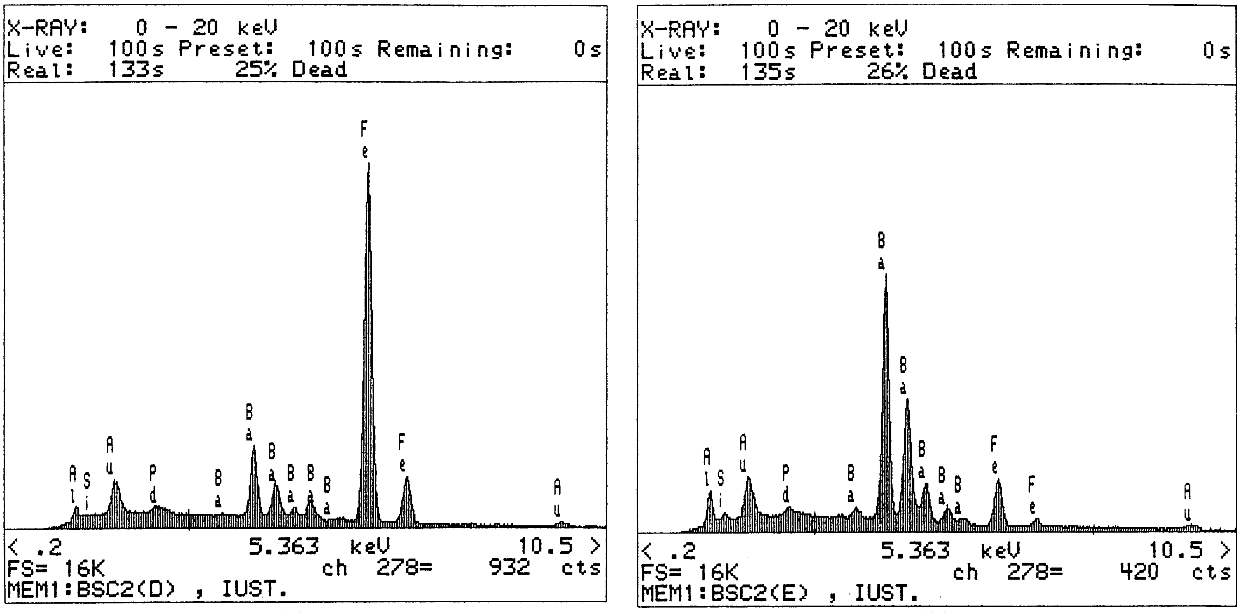

(a) (b)

Fig. 5. EDS analysis of glass specimen BSC1 (shown in Fig. 4), (a) Fe_2O_3-rich glass phase (bright) and (b)BaO and B_2O_3 (not shown)-rich phase (dark regions).

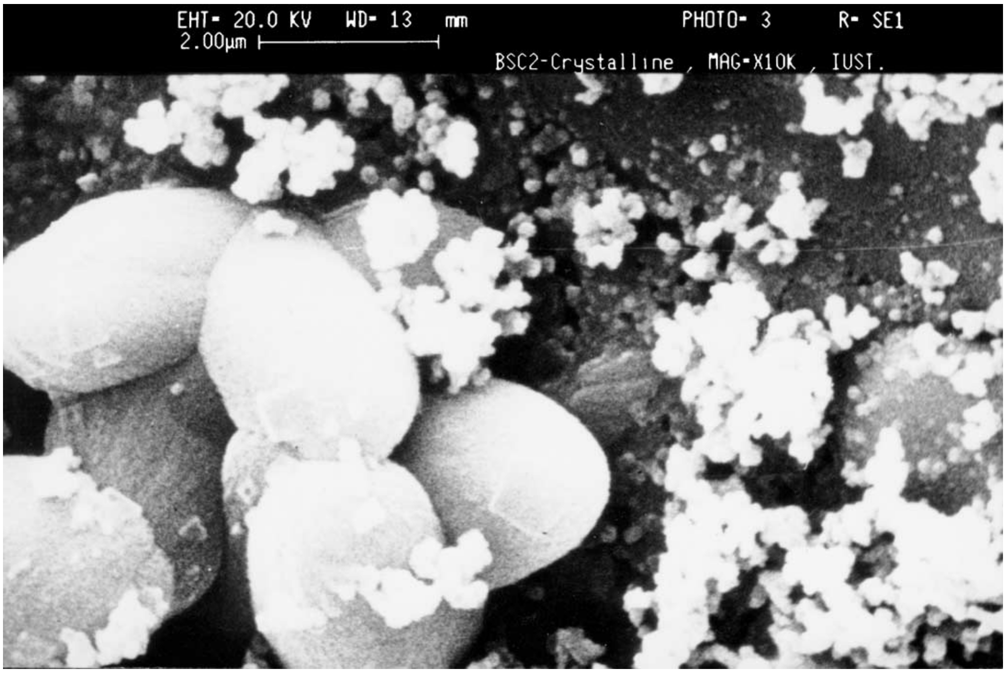

Fig. 6. SEM micrograph of glass specimen BSC1 after crystallisation at 723 °C for 1 h.

particles may either nucleate and grow direcly from glass surfaces or at the surface of previously crystallised $BaFe_{12}O_{19}$ particles. Although the precipitation of $BaFe_{12}O_{19}$ at the expense of iron oxide and barium borate microcrystallites has been reported by other investigators for relatively long heat treatment periods [18], considering the short crystallisation period in the present work it seems that $BaFe_{12}O_{19}$ particles were heterogeneously nucleated and grown at the borate particle surfaces. Fig. 9 shows the enlarged micrograph of barium hexaferrite platelets. The average diameter of particles is $< 0.5\mu_m$ and some reveal the hexagonal habit of $BaFe_{12}O_{19}$. Considering the fact that critical size of barium hexaferrite particles, below which the particles may magnetically be single domain has been reported to be 460 nm [19,20], it seems that particles precipitated

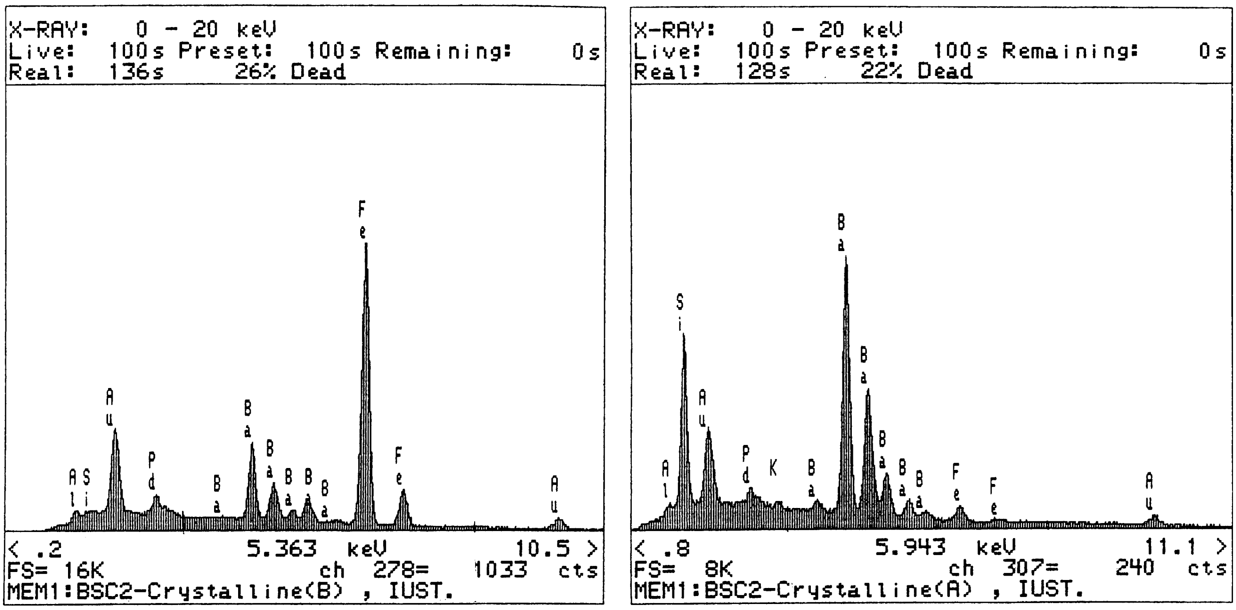

(a) (b)

Fig. 7. EDS analysis of glass specimen BSC1 after crystallisation (a) Ba-hexaferrite platelets, (b) BaB_2O_4 ellipsoids.

Fig. 8. Enlarged SEM micrograph of specimen BSC1 after crystallisation at 723 °C for 1 h, showing BaB_2O_4 ellipsoids.

from BSC1 specimens under the heat treatment conditions of the present study may be single domain. It may be concluded that the main role of Cr_2O_3 in the crystallisation process is the formation of a fine Fe_2O_3 rich phase via glass-in glass phase separation, surrounded by a B_2O_3 rich phase with a much coarser microstructure. $BaFe_{12}O_{19}$ particles formed within the Fe_2O_3 rich regions, owing to short diffusion distances, may crystallise very rapidly, but being surrounded by the $Ba_2O_3 + BaO$ rich phase which is very poor in Fe_2O_3, they should be confined within the boundaries of their respective region. The borate phase, on the other hand, may grow from the other separated glass phase, rich in Ba_2O_3 and BaO. It seems that the representation of a more comprehensive account of the crystallisation mechanism of glass specimens in this system, containing Cr_2O_3 as an additive, needs more research work.

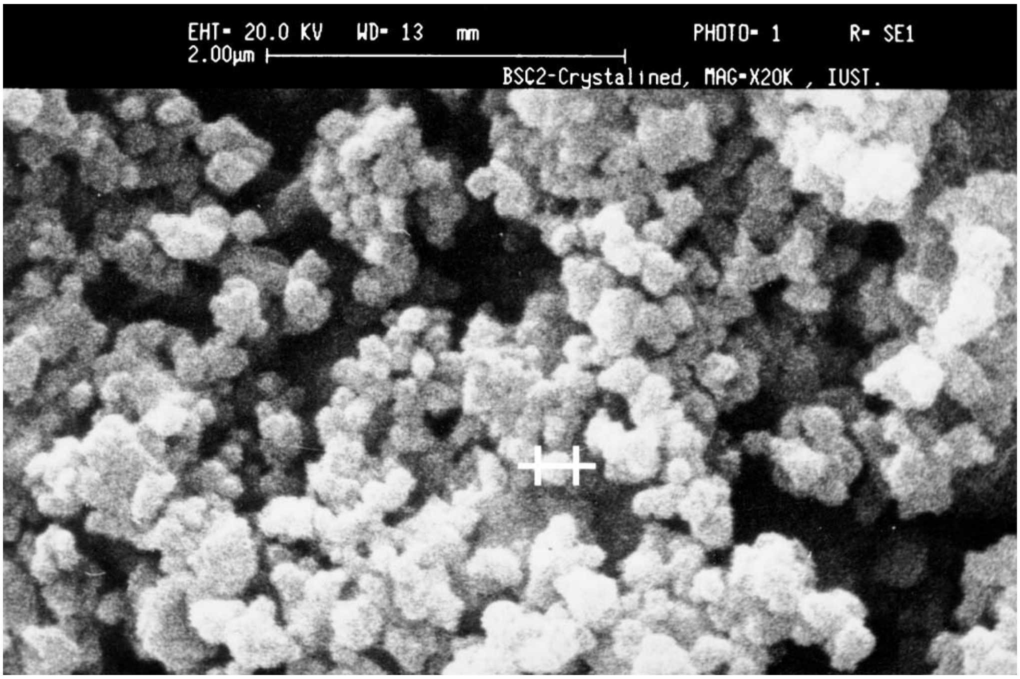

Fig. 9. Enlarged micrograph of specimen BSC1 after crystallisation exhibiting Ba-hexaferrite platelets.

3.3. Magnetic properties

Table 4 summarises the magnetic properties. The specimen BSC1 was prepared by sintering of pressed glass frits at the indicated temperature whereas the rest of specimens were produced by devitrification of bulk glass specimens. Figs. 10 and 11 show the particle size distribution and magnetisation curves respectively, for spesimen BSC1.It may be concluded that the specimen BSC1 exhibited much higher coercivity ($H_c = 4.15$ kOe) compared with other specimens investigated in the present work. This coercivity is quite high in comparison to the values reported in the literature for Ba-hexaferrite glass-ceramics in this system. This may be attributed to the shape and small size of Ba-hexaferrite particles [4,8,20]. However the effect of substitution of Cr^{3+} ions on the magnetic properties of $BaFe_{12}O_{19}$ should not be neglected, and needs further study. On the other hand the values of saturation magnetisation are relatively low for all specimens (including BSC1). Since the saturation magnetisation depends not only on particle size and shape but on the amount of magnetic phase relative to

Table 4
Magnetic properties obtained under a max. magnetic field of 20 kOe

Specimen	Heat treatment condition (°C/h)	H_c (Oe)	M_s (emu g^{-1})
BC1	809/3	1240	6.33
BS10	797/1	910	7.60
BS10	871/1	1050	7.60
BSC1	723/1	4150	9.92

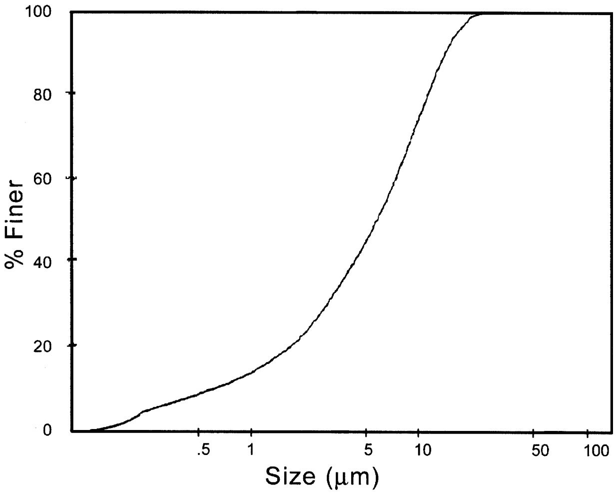

Fig. 10. Particle size distribution of BSC1 glass frit used in the fabrication of sintered specimens.

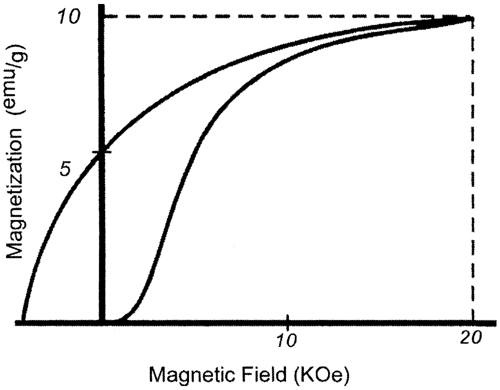

Fig. 11. Magnetisation curve of specimen BSC1 prepared by sintering and crystallisation of glass frits.

that of non-magnetic phase [9], considering the composition(which gives a maximum calculated amount of Ba-hexaferrite ~36%) it seems that the relatively low amount of Ba-hexaferrite phase is mainly responsible for the low value of saturation magnetisation.Therefore further effort is necessary to optimise the process, especially with respect to composition and heat treatment conditions.

4. Conclusions

The glass composition 45BaO–30Ba$_2$O$_3$–25Fe$_2$O$_3$ (mole%) prepared via glass-ceramic route, showed very weak bulk and surface crystallisation tendency. The addition of 1 mol% Cr$_2$O$_3$ to this composition greatly increased the bulk crystallisation tendency but make it susceptible to spontaneous crystallisation. Substitution of SiO$_2$ for Ba$_2$O$_3$, on the other hand, improved the bulk crystallisation ability, but led to the appearance of various silicate phases and in the case of >10 mol% SiO$_2$, prevented the formation of Ba-hexaferrite. Addition of 1 mol% Cr$_2$O$_3$ to the specimen containing 10 mol% SiO$_2$, while preventing the appearance of silicate phases, completely prohibited the bulk crystallisation process. The latter specimens on the other hand showed greatly enhanced surface crystallisation ability.

The glass-ceramic specimens made by the crystallisation of pressed glass frits containing 10 mol% SiO$_2$ and nucleated by 1% Cr$_2$O$_3$, developed Ba-hexaferrite and BaB$_2$O$_4$ as the only crystalline phases after a heat treatment of 1h at 723 °C. The latter specimens showed a quite high value of coercivity ($H_c = 4.15$ kOe) and relatively low value of saturation magnetisation ($M_S = 9.95$ emu/g).

References

[1] B.T. Shirk, W.R. Buessem, Magnetic properties of barium ferrite formed by crystallisation of a glass, J. Am. Ceram. Soc. 53 (4) (1970) 192–196.

[2] O. Kubo, T. Ido, H. Yokoyama, Properties of barium ferrite particles for perpendicular magnetic recording medias, IEEE Trans. Magn. Mag-18 (6) (1982) 1122–1124.

[3] H. Zagnazi, C. Chaumont, J.C. Bernier, Rules for the preparation of powders by the glass synthesis method—Application to barium hexaferrite, J. Solid State Chem. 65 (1986) 370–376.

[4] K. Oda, T. Yoshio, K.O. Oka, Morphology and magnetic properties of BaFe$_{12}$O$_{19}$ particles prepared by the glass-ceramic method, J. Mater. Sci. Lett. 20 (4) (1985) 876–879.

[5] F. Haberey, Preparation of M and W-type hexaferrite particles by the glass crystallisation method on the basis of the pseudo-ternary system Fe$_2$O$_3$–BaO–B$_2$O$_3$, IEEE Trans. Magn. Mag-23 (1) (1987) 29–32.

[6] S. Ram, D. Bahadur, D. Chakravorty, Magnetic glass-ceramics with hexagonal lead ferrites, J. Non-Cryst. Solids 88 (1986) 311–322.

[7] S. Ram, D. Bahadur, D. Chakravorty, Crystallisation of W-type hexagonal ferrites in an oxide glass with As$_2$O$_3$ as nucleation catalyst, J. Magn. Magn. Mater. 67 (1987) 378–386.

[8] P. Brahma, K. Choudhury, R. Guha, D. Chakravorty, Crystallisation of Ba-M ferrite in a glass with Sb$_2$O$_3$ as nucleation catalyst, J. Mater. Sci. Lett. 24 (8) (1989) 540–542.

[9] C.K. Lee, R.F. Speyer, Glass formation and crystallisation of barium ferrite in the Na$_2$O–BaO–Fe$_2$O$_3$–SiO$_2$ system, J. Mater. Sci. 29 (1994) 1348–1351.

[10] U.C. Johri, R.M. Singru, D. Bahadur, Mössbauer spectroscopic studies of glass ceramics with hexagonal barium and strontium ferrites, J. Mater. Sci. 27 (1992) 6223–6228.

[11] C.K. Lee, Y. Berta, R.F. Speyer, Effect of Na$_2$O addition in the crystallisation of barium ferrite from a BaO–B$_2$O$_3$–Fe$_2$O$_3$ glass, J. Am. Ceram. Soc. 79 (1) (1996) 183–192.

[12] R. Müller, C. Ulbrich, W. Schüppel, H. Steinmetz, E. Schuppel, H. Steinmetz, E. Steinbeiß, Prepartion and properties of Ba-ferrite containing glass ceramics, J. Eur. Ceram. Soc. 19 (1999) 1547–1550.

[13] K. Watanabe, K. Hoshi, Crystallisation kinetics of fine barium hexaferrite, BaFe$_{12}$O$_{19}$, particles in a glass matrix, Phys. Chem. Glasses 40 (2) (1999) 75–78.

[14] O.V. Mazurin, G.P. Roskova, Properties of phase separated glasses, in: O.V. Mazurin, E.A. Porai-Koshits (Eds.), Phase Separation in Glass, North Holland, Amsterdam, 1984, pp. 249–262.

[15] S.W. Freiman, G.X. Onoda Jr., A.G. Pincus, Spherulitic crystallisation in glasses, in: L.L. Hench, S.W. Freiman (Eds.), Advances in Nucleation and Crystallisation in Glasses, Am. Ceram. Soc., Columbus OH, 1971, pp. 144–150.

[16] H.D. Keith, F.J. Padden Jr., A phenomenological theory of spherulitic crystallisation, J. Appl. Phys. 34 (8) (1963) 2409–2421.

[17] S.W. Freiman, G.Y. Onoda Jr., A.G. Pincus, Controlled crystallisation in 3BaO–5SiO$_2$ glass, J. Am. Ceram. Soc. 55 (7) (1972) 354–359.

[18] S. Ram, D. Chakravorty, D. Bahadur, Effect of nucleating agents on the crystallisation behaviour of barium hexaferrite in a borate glass, J. Magn. Magn. Mater. 62 (1986) 221–232.

[19] N. Rezlescu, L. Rezlescu, M.L. Craus, E. Rezlescu, Magnetic glass-ceramic containing fine ferrite crystals, J. Magn. Magn. Mater. 196-197 (1999) 463–464.

[20] L. Rezlescu, E. Rezlescu, P.D. Popa, N. Rezlescu, Fine barium hexaferrite powder prepared by the crystallisation of glass, J. Magn. Magn. Mater. 193 (1999) 288–290.